Effects of Contamination on WFPC2 Photometry

Brad Whitmore, Inge Heyer, and Sylvia Baggett
June 14, 1996

ABSTRACT

Photometric monitoring observations are examined to determine the effect of contamination on WFPC2 photometry. New contamination rates are determined using observations of both a white dwarf standard (GRW+70D5824) and a globular cluster (Omega Cen = NGC 5139). Evidence for a long term increase in throughput with time has been found on the PC1 for F160BW and F170W filter observations. This, and other supporting evidence from the thermal vacuum tests and on-orbit observations, suggest that a long-lived contaminant is present in the PC1 which is slowly dissipating. In addition, corrections to the relative zeropoints for the different chips are determined for the F160BW, F170W, and F218W filters.

1. Introduction

Contaminants in the WF/PC-1 severely limited it's UV capabilities. During the construction of WFPC2, great care was taken to minimize the effects of contamination. This has been largely successful, increasing the 50% throughput loss time at about 1600 Angstroms from less than a day with WF/PC-1 (F194W filter) to roughly 40 days with WFPC2 (F160BW filter). However, the effects of contamination are clearly present on the WFPC2 and it is the goal of this Instrument Science Report (ISR) to help characterize these effects. This ISR adds to, and supersedes some of the results presented in ISR WFPC2 96-02 "Contamination Correction in SYNPHOT for WFPC2 and WF/PC-1," which focused on changes to SYNPHOT, the synthetic photometry package.

2. Monthly Contamination Cycle

The UV throughput of the WFPC2 degrades in a predictable way after each monthly decontamination. Figure 1 shows the photometric monitoring data for the spectrophotometric standard star GRW+70D5824 (a white dwarf classified DA3; B-V = -0.09) in the WF3 and PC1 for the set of filters which are routinely monitored. The dotted vertical lines mark decontamination dates. The solid vertical lines mark the date the operating temperature was changed from -76^{o}C to -88^{o}C; the information provided here is for the period following the cooldown date (April 24, 1994). The figure illustrates that the effect of contamination on the F675W and F814W filter observations is essentially negligible, but rises toward the UV until it reaches values of 30 - 40% per month for the F160BW filter.

Table 1 shows the monthly throughput declines measured from this data. The values in parentheses are based on similar observations of the globular cluster Omega Cen (NGC 5139; mean B-V ~ 0.7 mag). In general, the values derived from the Omega Cen data are in good agreement with the values derived from GRW+70D5824 data.

Table 1: Throughput Decline Rates over 30 Days

Filter	PC1	+/-	WF2	+/-	WF3	+/-	WF4	+/-
F160BW	-0.263	0.030	-0.378	0.090	-0.393	0.051	-0.381	0.066
F170W	-0.160	0.011	-0.284	0.005	-0.285	0.006	-0.232	0.006
F218W	-0.138	0.009	-0.226	0.015	-0.255	0.010	-0.213	0.033
F255W	-0.070	0.007	-0.136	0.017	-0.143	0.009	-0.108	0.042
F336W	-0.016 (-0.038)	0.008 (0.018)	(-0.043)	(0.010)	-0.057 (-0.046)	0.011 (0.008)	(-0.047)	(0.007)
F439W	-0.002 (0.002)	0.007 (0.014)	(-0.022)	(0.007)	-0.021 (-0.023)	0.010 (0.009)	(-0.023)	(0.007)
F555W	-0.014 (0.007)	0.006 (0.013)	(-0.007)	(0.007)	-0.016 (-0.009)	0.008 (0.009)	(-0.008)	(0.008)
F675W	-0.001 (-0.020)	0.006 (0.020)	(0.001)	(0.011)	-0.001 (0.002)	0.006 (0.011)	(0.004)	(0.011)
F814W	0.007 (0.013)	0.007 (0.019)	(-0.002)	(0.009)	0.003 (-0.000)	0.008 (0.009)	(-0.002)	0.016 (0.010)

Note 1 - The Omega Cen data (in parenthesis) was determined using stars within 300 pixels of the CCD centers, hence are most representative for a mean position 212 pixels from the center. Analysis of the F336W Omega Cen data suggests slightly higher rates (roughly 0.13 mag) of contamination toward the center. See section 3 for details.

Note 2 - The GRW+70D5824 observations were taken at the center of PC1, but at a position roughly 17” in X and Y from the pyramid apex for the WF chips.

Note 3 - 0.5” radii apertures were used for GRW+70D5824 data. 3 pixel radii apertures were used for the Omega Cen data (0.14” for PC and 0.3” for WF).

Figure 1: Photometric monitoring data for WFPC2.

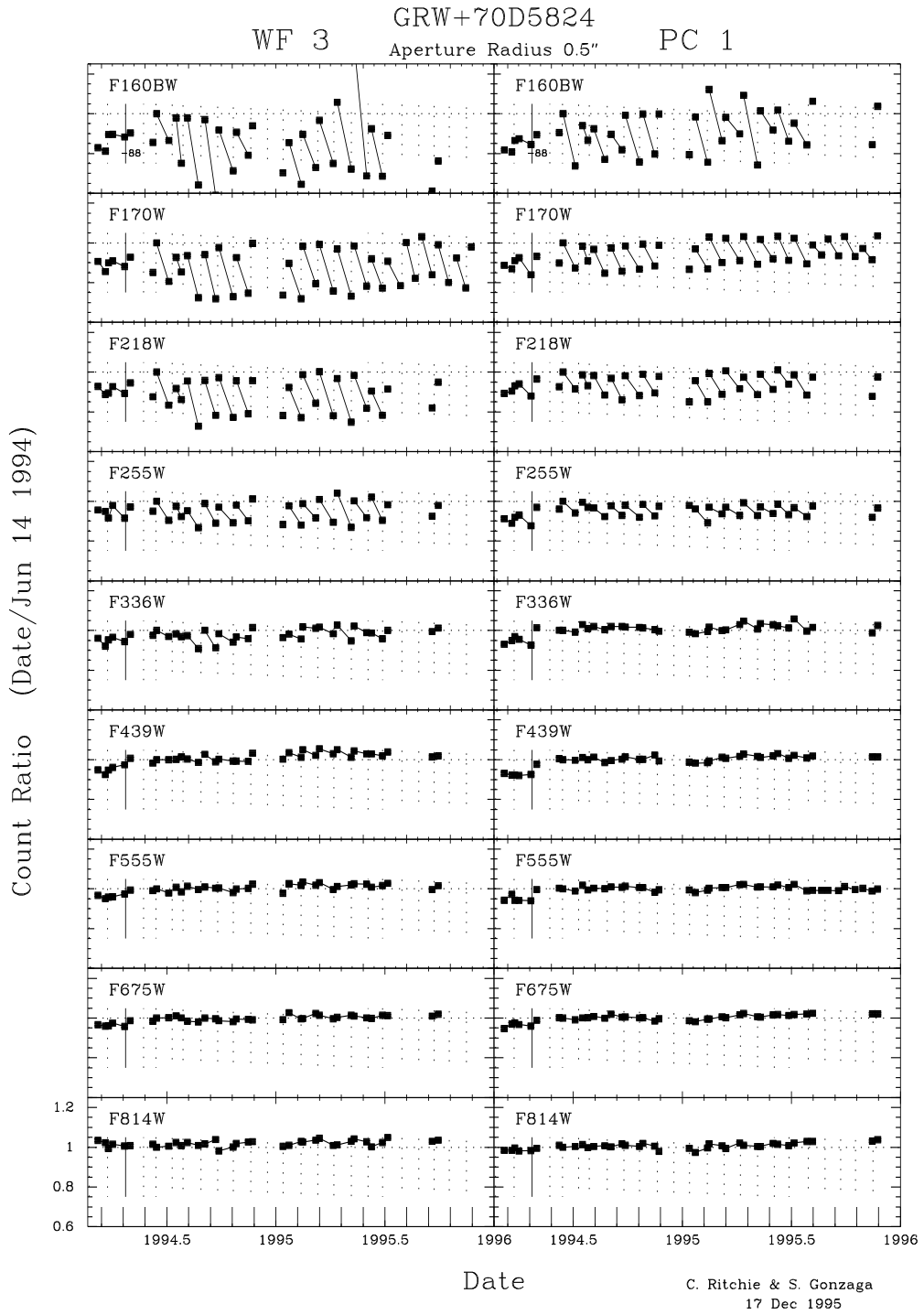

Figure 2 shows the throughput decline in all four chips as a function of days since the last decontamination for the F170W filter. The contamination rate is remarkably constant and can be accurately modeled by a simple linear decline in throughput following the decontamination, which appears to return the throughput to roughly the nominal value each month. While the contamination rates are similar for the three WF chips, the values for the PC are generally about half as large. In addition, there is evidence for a long term increase in throughput on the PC1. These results will be discussed in Section 6.

Figure 2: Throughput with the F170W filter following Decontaminations. Separate lines are fit to the data before and after Jan 1,1995.

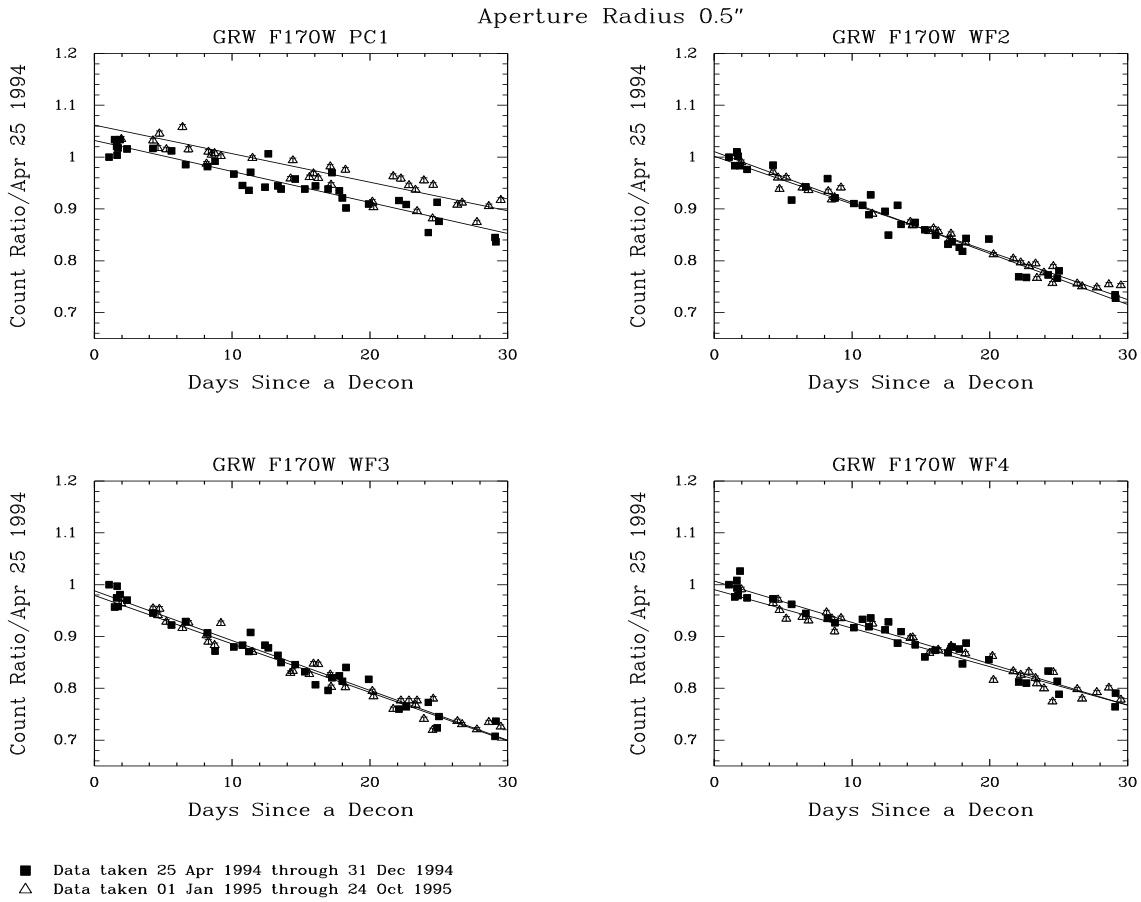

The decline in throughput appears to be due primarily to scattering of light rather than absorption, based on two observations. First, as discussed in ISR WFPC2 96-02, analysis of the light level off the edge of the pyramid shows that most of the missing light is scattered. In addition, the fact that the variation in the F336W VISFLAT observations due to the monthly contamination cycle is about 1.5 % (ISR WFPC2 96-01), while the variation in aperture measurements of stars is about 4.5 %, suggests that most of the variation is due to scattering. The scattering removes the light from the aperture for point sources, but since it generally redistributes it elsewhere on the CCD, measurements of uniformly illuminated sources (e.g. the VISFLAT lamp) are not affected as much.

3. Spatial Dependence of the Monthly Contamination

Analysis of the F336W data for Omega Cen data show a small dependence of the contamination rate on the location of the star on the chip, in the sense that the contamination rate over 30 days in the center is larger by about 0.024 +/- 0.008 mag than at a position 400 pixels from the center, based on linear fits to the data. The effect is seen on all four chips and the uncertainty represents the scatter between the chips. However, these results should be considered as tentative for the present, since the F336W, with only about 5% monthly contamination, is not optimal for this test. More sensitive observations will be taken in Cycle 6 (Photometric Transformation calibration proposal, #6935) when NGC 2100, a young cluster in the LMC, will be used to map out the contamination rate in the F255W, F170W, and F160BW filters.

4. Spectral Dependence caused by Red Leaks

A slight difference between the throughput declines for GRW+70D5824 and Omega Cen might be expected due to differences in spectral shape, especially for filters like F336W which have a substantial redleaks. However, even in the case of F336W, the effect should be less than 0.01 mag based on SYNPHOT simulations (B-V=-0.09 for GRW+70D5824 and B-V ~ 0.7 for Omega Cen). Figure 3 shows the SYNPHOT predicted contamination declines in F336W as a function of B-V for all targets in the BPGS catalog.

Figure 3: SYNPHOT contamination correction for F336W as a function of B-V.

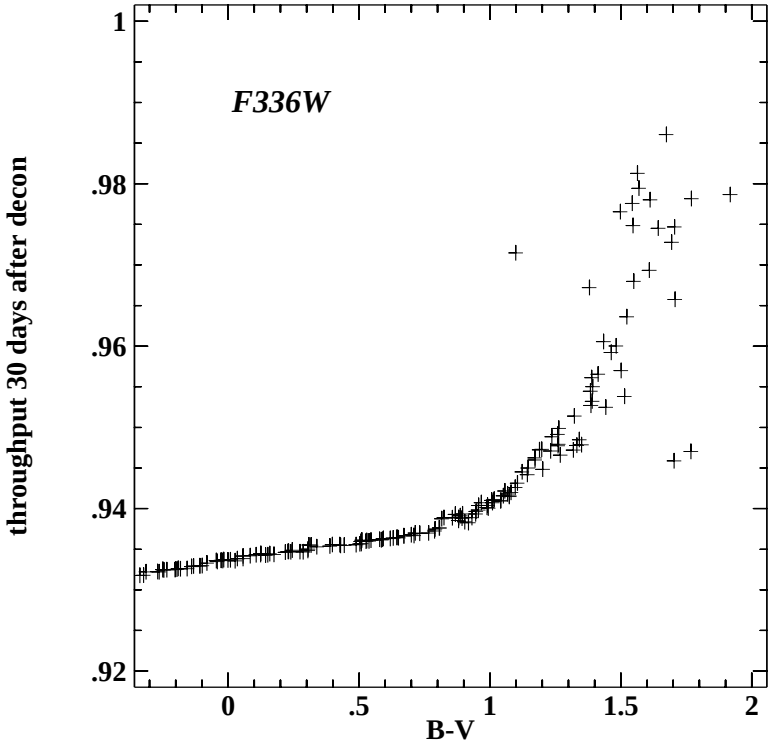

Deriving the Contamination Correction using SYNPHOT

To compute an estimate of the contamination correction, SYNPHOT's calcphot task may be used along with an appropriate spectrum. Here, we used the Bruzual-Persson-Gunn-Stryker atlas; these spectra (as well as others) are available from STScI via ftp as well as the WWW (see References). To compute the estimated throughput decline, calcphot is run twice, once for a date right after a decon procedure and once for 30 days later. Since the same throughput decline is implemented for every decon period (see ISR WFPC2 96-02), the MJD used in calcphot can be that for any decon. Here, the July 28,1994 decon date was used (49561.3; iraf commands are italicized):

calcphot "wfpc2,2,f336w,a2d7,cal,cont#49561.3" bpgs_16.tab form=counts

```
Mode = band(wfpc2,2,f336w,a2d7,cal)
   Pivot       Equiv Gaussian
 Wavelength          FWHM
  3358.735        479.4135    band(wfpc2,2,f336w,a2d7,cal)
Spectrum:  /tib/cdbs/grid/bpgs/bpgs_16.tab
    VZERO      (COUNTS s^-1 hstarea^-1)
       0.           6.1871E7
```

calcphot "wfpc2,2,f336w,a2d7,cal,cont#49591.3" bpgs_16.tab form=counts

```
Mode = band(wfpc2,2,f336w,a2d7,cal,cont#49591.3)
   Pivot       Equiv Gaussian
 Wavelength          FWHM
  3361.844         485.799    band(wfpc2,2,f336w,a2d7,cal,cont#49591.3)
Spectrum:  /tib/cdbs/grid/bpgs/bpgs_16.tab
    VZERO      (COUNTS s^-1 hstarea^-1)
       0.           5.7769E7
```

yielding a throughput decline of ~0.935. The B-V values for the BPGS spectra are available via WWW but can also be obtained from the table header, e.g,

tdump bpgs_16.tab cdfile=STDOUT pfile=STDOUT datafile=STDOUT row=1

```
WAVELENGTH       R          %12.4g  Angstroms
FLUX             R          %12.4g  FLAM
STATERROR        R          %12.4g  FLAM
SYSERROR         R          %12.4g  FLAM
FWHM             R          %12.4g  Angstroms
DESCRIP  t Bruzual-Persson-Gunn-Stryker Spectra Library
DBTABLE  t CRGRID
SOURCE   t BPGS Library
TARGETID t HR6169
OBSMODE  t
MKTYPE   t A2V
AV       r 0.067
V        r 6.373
U-B      r 0.177
B-V      r -0.017
V-R      r -0.203
R-I      r -0.246
V-K      r -0.040
COMMENT  t BPGS Star Number   16
COMMENT  t SPECTRA HAVE BEEN NORMALIZED TO V=0
COMMENT  t IR distributions from Strecker et al (ApJS 41, 501, 1979)
COMMENT  t And other unpublished sources.
```

```
COMMENT  t IR and Optical data were tied together by the V-K colors
COMMENT  t Data converted from BPGS library format to STSDAS table
COMMENT  t by K D Kuntz
HISTORY  t Created Thu 13:13:24 05-Apr-90
COMMENT  t Spectral types are taken from Gunn and Stryker
COMMENT  t paper, ApJ Supplement 52:121-153, 1983 June
         229.            0.         INDEF         INDEF         INDEF
```

...

5. Dependence on Aperture

There is very good agreement in the contamination rates obtained using apertures that range in size from 1 to 5 pixel radii, based on the Omega Cen data for F336W. The scatter in the 30 day contamination rates for the four determinations (aperture with radii 1,2,3 and 5 pixels) for the PC is 0.013 mag, and for the WF is just 0.0012 mag. Table 3 used apertures with 0.5” radii for the GRW+70D5824 measurements while 3 pixel radii were used for the Omega Cen data (0.14” for PC and 0.3” for WF).

Version 3 of the WFPC2 Instrument Handbook (Burrows et. al, 1995) indicates that contamination rates as high as 5% per month have been measured from GRW+70D5824 data at F555W on the WF using very large 3” (30 pixel) radii. The Omega Cen data is in the process of being checked for this effect; results will be presented in a later report. In any case, the small aperture measurements reported here and elsewhere should be much less susceptible to a variety of effect such as CTE and digitization noise. We conclude that the 30 day contamination rate at F555W is only 1 or 2 %.

6. Long Term Throughput Variations

In addition to the monthly changes in throughput discussed in section 2, there is now evidence for long term variations, especially for the F170W data on the PC1 where the throughput has increased at the rate of about 5 % per year. This is evident in Figure 1, but is much clearer in Figure 2 where the data before and after Jan 1, 1995 are compared, and in Figure 4 where the effect of the monthly decontamination is removed and the dependence with time (MJD = Modified Julian Date) is shown. The F160BW filter shows an even stronger trend but with larger uncertainties.

Figure 4: Change in Throughput as a Function of Time[1].

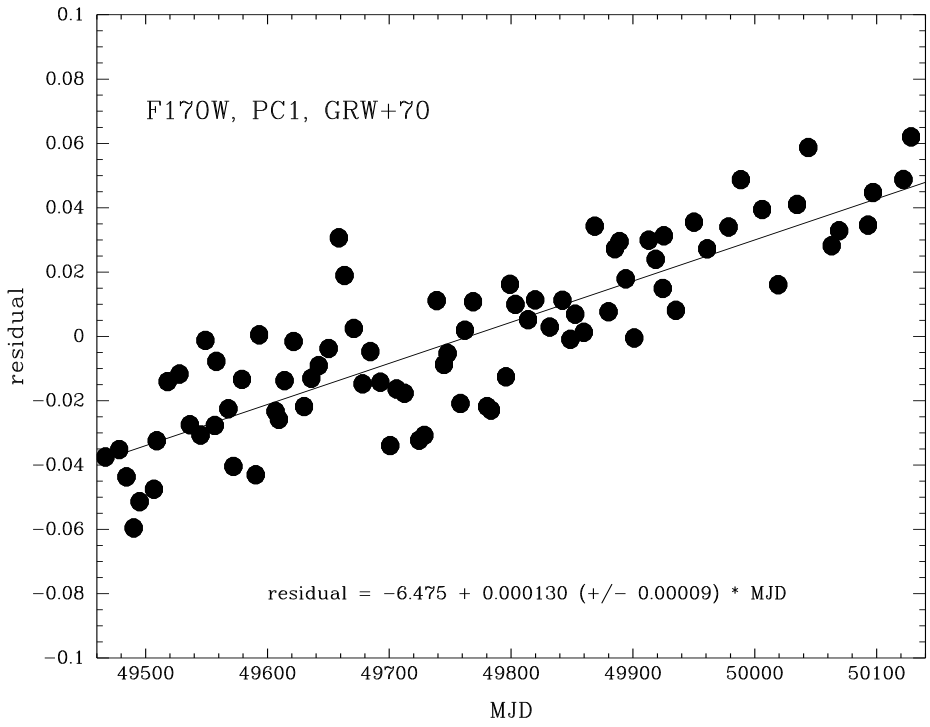

Table 2 shows the change in throughput for the standard set of filters, after the effect of the monthly decontamination is removed. The WF chips show much weaker trends in the opposite sense in F160BW and F170W (i.e., throughput decreasing slightly with time).

The other filters generally show small increases in throughput based on the GRW+70D5824 data, but small decreases based on the Omega Cen data. Although the results are in agreement for the WF3 observations for F336W, we consider this tentative since similar trends are not seen for the F255W and F439W data. Hence, at present, only the increases for F170W and F160BW on PC1 are considered firm results.

1. Determined after removing the effects of the monthly decontamination.

Table 2: Changes in Throughput in One Year.[a]

Filter	PC1		WF2		WF3		WF4	
F160BW	0.090	0.017			-0.034	0.038		
F170W	0.048	0.003	-0.003	0.003	-0.009	0.003	-0.013	0.003
F218W	0.014	0.007			-0.003	0.008		
F255W	-0.005	0.005			0.011	0.006		
F336W	0.010 (-0.030)	0.006 (0.014)	(-0.015)	(0.009)	-0.023 (-0.018)	0.007 (0.006)	(-0.022)	(0.007)
F439W	0.016 (-0.018)	0.005 (0.011)	(0.000)	(0.006)	0.024 (-0.013)	0.006 (0.007)	(-0.009)	(0.006)
F555W	0.003 (-0.017)	0.004 (0.013)	(-0.011)	(0.007)	0.016 (-0.012)	0.005 (0.009)	(-0.014)	(0.008)
F675W	0.017 (-0.012)	0.004 (0.018)	(+0.010)	(0.010)	0.012 (+0.002))	0.004 (0.011)	(-0.016)	(0.009)
F814W	0.018 (-0.029)	0.005 (0.015)	(+0.002)	(0.009)	0.019 (-0.011))	0.005 (0.008)	(-0.013)	(0.009)

a. Long term throughput change after monthly decontamination effects are removed. Values in parentheses are from the Omega Cen observations; dark shading highlights where non-zero values are clearly present. The photometric calibration in the WFPC2 Instrument Handbook, the HST Data Handbook, and the image headers (PHOTFLAM, determined from SYNPHOT) are appropriate for 1994.5. At that time, a comparison between observed data and the SYNPHOT predictions showed a mean ratio of 0.987 with a scatter of 0.025, based on 32 filters ranging from F160BW to F1042M (Whitmore, 1995).

What causes the increase in the F160BW and F170W throughputs on the PC1? An increase in the red leak seems unlikely since both filters show a decrease only in PC1. In addition, preliminary results based upon on-orbit VISFLATs show that although new pinholes have developed since the Thermal Vacuum test (private communication, J. Clarke, 1996) no new pinholes have developed during orbit in F160BW and that the flux through the current pinholes has not increased more than ~10% in WF2 (the worst chip; M.Stiavelli, 1996).

The most likely explanation is that there is a long-lived contaminant in the PC1 which is only now slowly dissipating. There are several pieces of evidence that support this idea. First, Table 7.5 in the Thermal Vacuum Report (Trauger et al., 1993) shows that the count rates in the PC are roughly a factor of two lower than on the WF for the Xenon lamp (monochromatic emission at 1470 Angstroms) and roughly 40 % lower for the Deuterium lamp observed with the F170W filter. In the report, this was attributed to nonuniform illumination and possible chromatic aberration of the illuminating source, since the CCUV (calibration channel UV lamp) did not show similar effects (although there is also a 10 % decrease in the F170W observations for this lamp). However, it seems unlikely that nonuniformities in the illumination pattern are large enough to cause the effect, particularly

for the Xenon lamp where Figures 7.3 and 7.4 (Trauger et al., 1993) suggests relatively similar levels of contamination for PC1 and WF2. While the illumination of WF3 and WF4 appear to be more severely affected, explaining the 10 - 20 % spread differences seen between the WF's, the factor of two or more needed to explain the WF to PC ratios in Table 7.5 (Trauger et al., 1993) is difficult to understand unless contamination in the PC1 is present.

Another piece of circumstantial evidence for a long-live contaminant is that the contamination rates on the PC1 are roughly half the WF rates, as shown in Figures 1 and 2 and Table 1. This might be expected if a long term contaminant is present on PC1 which acts to repel the short term contaminant responsible for the monthly declines. This repulsion effect may be seen in the "worm" features on WF2 (WFPC2 ISR 95-06, Chapter 6). The lower absolute count rates for the GRW+70D5824 observations on PC1 in F170W are perhaps the most direct evidence (see next section), although questions about the quality of the flat fields introduce some uncertainty, as will be discussed in the next section.

7. Zeropoint Corrections for F160BW, F170W, and F218W

If long term contaminants are responsible for the improving throughput on the PC1 for the F160BW and F170W filters, we would expect the absolute number of counts in the PC to be lower than in the WF chips. This is indeed the case, as shown in Table 3, with the difference ranging from 9% in F160BW for WF3 to 19% in F170W for WF2. The results for the F160BW filter are nearly identical. However, this raises another interesting point. For filters blueward of F255W, the variance in the counts for the three WF chips is much larger than would be expected if the flatfields are normalizing the chips, as they are designed to do. A normalization problem can not be ruled out; it is very difficult to make flats in the UV since the Earth is too faint to provide a good flat field. The current UV flats were made by assuming that the UV lamp provided a uniform illumination.

Table 3: Zeropoints for Point Sources.[a]

Filter	PC1	+/-	WF2	+/-	WF3	+/-	WF4	+/-
F160BW	0.909	0.015	1.179	0.062	1.000	0.030	1.091	0.054
F170W	0.920	0.006	1.187	0.005	1.000	0.005	1.062	0.005
F218W	1.082	0.005	1.066	0.008	1.000	0.009	1.093	0.023
F255W	1.025	0.004	1.012	0.010	1.000	0.009	0.994	0.027

a. Divide your observed count rates by these values, or equivalently, divide your value of PHOTFLAM from the header (used to determine the photometric zeropoint), in order to provide approximate corrections for shortcomings in the far UV flat fields. These values are normalized to 1994.5, and for the gain = 14 setup. See Table 2 to correct for long term changes in the throughput of F160BW and F170W observations.

In any case, we recommend using the zeropoints listed in Table 3 for F160BW, F170W, and F218W until new flats become available. It should also be kept in mind that these zeropoints are for observations of stars at positions roughly 24” from the apex of the pyramid in each chip. The spatial dependence of this correction is essentially unknown, although there is a hint from the F336W observations of Omega Cen (Section 3) that it may be quite nonuniform. The Cycle 6 Photometric Transformation calibration program (#6935; see also WFPC2 Instrument Handbook, v.4, pg 185) will use observations of a blue cluster in the LMC to make this determination.

It is possible that the differences in the absolute count rates for the GRW+70D5824 observations on the different chips are due to “static” contamination rather than shortcomings in the flat fields. However, the absence of any long term dependence on the WF chips makes this explanation seem unlikely.

8. Summary

To summarize, we recommend the following procedure to correct for contamination in WFPC2 data.

Step # 1 - Use Table 1 to correct the throughput for monthly contamination. This is probably not necessary on the PC redward of F336W, or on the WFs redward of F555W. Table 4 at the end of this report lists the decontamination dates through May 1996, or check the online WFPC2 history file (see References for URL).

Step # 2 - Use Table 2 to correct for long term contamination for PC observations done with the F160BW or F170W filters, so as to obtain the effective 1994/1995 countrates.

Step # 3 - Use Table 3 to correct the zeropoint for observations with F218W and blueward. We will announce any changes to the UV flatfields that supersedes this advice and update the online WFPC2 history file as well.

Note that at present we are not recommending a correction for spatial dependencies since they are not yet well determined. Our Cycle 6 calibration program should provide the data necessary for making this determination, and for improving many of the numbers contained in this ISR.

Table 4: Dates of WFPC2 Decontamination Procedures[2]

year	date	day of year	modified Julian date	year	date	day of year	modified Julian date
1994	22 Feb 11:37	053	49405.4840	**1995**	7 May 01:13	127	49844.0507
	24 Mar 11:08	083	49435.4639		2 Jun 18:30	153	49870.7708
	24 Apr 00:49	114	49466.0340		27 Jun 20:00	178	49895.8333
	23 May 15:00	143	49495.6250		30 Jul 08:50	211	49928.3681
	13 Jun 11:02	164	49516.4597		27 Aug 05:43	239	49956.2382
	10 Jul 11:40	191	49543.4861		22 Sep 03:40	265	49982.1528
	28 Jul 07:12	209	49561.3000		17 Oct 09:43	290	50007.4053
	27 Aug 09:46	239	49591.4069		15 Nov 08:53	319	50036.3706
	25 Sep 00:46	268	49620.0319		14 Dec 07:03	348	50065.2929
	21 Oct 00:41	294	49646.0285	**1996**	11 Jan 23:24	011	50093.9750
	19 Nov 17:29	323	49675.7285		11 Feb 00:30	042	50124.0208
	18 Dec 06:00	352	49704.2500		10 Mar 00:21	070	50152.0147
1995	13 Jan 16:14	013	49730.6764		02 Apr 00:16	093	50175.0111
	12 Feb 01:54	043	49760.0792		04 May 17:09	125	50207.7146
	11 Mar 14:30	070	49787.6042		28 May 06:16	149	50231.2614
	8 Apr 10:29	098	49815.4368				

9. Acknowledgements ...

We thank John Biretta, Chris Burrows, John Clarke, John MacKenty, Massimo Stiavelli, and members of the WFPC2 group for helpful comments.

10. References[3]

Baggett, S., Sparks, W., Ritchie, C., MacKenty, J., “Contamination Correction in Synphot for WFPC2 and WF/PC-1”, Feb 1996, ISR WFPC2 96-02.

Biretta, J., et al., WFPC2 Instrument Handbook, Version 4.0, June 1996.

2. Note: decontamination procedures are 6 hours in length, except for Jun, July, Sep, and Oct 1994 (12 hours) and May 1994 (5.5 hours).
3. Paper copies of any of these reports may be obtained by contacting help@stsci.edu.

Biretta, J., Ritchie, C., and Rudloff, K., “A Field Guide to WFPC2 Image Anomalies,” Nov 1995, ISR WFPC2 95-06.

Burrows, C., et. al., WFPC2 Instrument Handbook, Version 3.0, June 1995.

Bushouse, H., “Synphot User’s Guide,” STSDAS Version1.3.3, March 1995.

Clarke, J., private communication, 1996.

Holtzman, J., Hester, J., Casertano, S., Trauger, J., Ballester, G., Burrows, C., Clarke, J., Crisp, D., Gallegher, J., Griffiths, R., Hoessel, J., Mould, J., Scowen, P., Stapelfeldt, K., Watson, A., and Westphal, J., “The Performance and Calibration of the WFPC2”, PASP **107**,156 (1995a).

Holtzman, J., Burrows, C., Casertano, S., Hester, J., Trauger, J., Watson, A., Worthey, G., “The Photometric Performance and Calibration of WFPC2” PASP, **107**, 1065(1995b).

MacKenty, J., and Ritchie, C., “WF/PC-1 Photometric Monitoring Results,” Feb 1993, ISR WF/PC-1 93-02.

Stiavelli, M., private communication, 1996.

Stiavelli, M., and Baggett, S., “Internal Flat Field Monitoring,” Jan 1996, ISR WFPC2 96-01.

Trauger et al., WFPC2 Investigation Definition Team, Prelaunch Thermal Vacuum Test Report, Nov 1993.

Whitmore, B., “Photometry with the WFPC2,”, in Proceedings from “Calibrating the Hubble Space Telescope: Post Servicing Mission,” May 1995 Workshop, Koratkar, A., and Leitherer, C., eds., pg 269.

WWW

The WFPC2 Documentation page, including links to the Thermal Vac Test Report, WFPC2 History File, ISRs, Monitoring and Synphot related memos, is at
http://www.stsci.edu/ftp/instrument_news/WFPC2/wfpc2_doc.html

Links to STScI’s online spectral atlases can be found at
http://www.stsci.edu/ftp/instrument_news/Observatory/astronomical_catalogs.html

Online STSDAS manuals (including SYNPHOT) are at
http://ra.stsci.edu/STSDAS.html